

Design Summary of the Mark-I Pebble-Bed, Fluoride Salt–Cooled, High-Temperature Reactor Commercial Power Plant

Charalampos Andreades,* Anselmo T. Cisneros, Jae Keun Choi, Alexandre Y. K. Chong, Massimiliano Fratoni, Sea Hong, Lakshana R. Huddar, Kathryn D. Huff, James Kendrick, David L. Krumwiede, Michael R. Laufer, Madicken Munk, Raluca O. Scarlat, Nicolas Zweibaum, Ehud Greenspan, Xin Wang, and Per Peterson

University of California, Berkeley, Nuclear Engineering Department, 4118 Etcheverry Hall, Berkeley, California 94720

Received January 8, 2016

Accepted for Publication March 25, 2016

<http://dx.doi.org/10.13182/NT16-2>

Abstract — *The University of California, Berkeley (UCB), has developed a preconceptual design for a commercial pebble-bed (PB), fluoride salt–cooled, high-temperature reactor (FHR) (PB-FHR). The baseline design for this Mark-I PB-FHR (Mk1) plant is a 236-MW(thermal) reactor. The Mk1 uses a fluoride salt coolant with solid, coated-particle pebble fuel. The Mk1 design differs from earlier FHR designs because it uses a nuclear air-Brayton combined cycle designed to produce 100 MW(electric) of base-load electricity using a modified General Electric 7FB gas turbine. For peak electricity generation, the Mk1 has the ability to boost power output up to 242 MW(electric) using natural gas co-firing. The Mk1 uses direct heating of the power conversion fluid (air) with the primary coolant salt rather than using an intermediate coolant loop. By combining results from computational neutronics, thermal hydraulics, and pebble dynamics, UCB has developed a detailed design of the annular core and other key functional features. Both an active normal shutdown cooling system and a passive, natural-circulation-driven emergency decay heat removal system are included. Computational models of the FHR—validated using experimental data from the literature and from scaled thermal-hydraulic facilities—have led to a set of design criteria and system requirements for the Mk1 to operate safely and reliably. Three-dimensional, computer-aided-design models derived from the Mk1 design criteria are presented.*

Keywords — *FHR, compact integral effects test, nuclear air-Brayton combined cycle.*

Note — *Some figures may be in color only in the electronic version.*

I. INTRODUCTION

This summary paper describes work performed at the University of California, Berkeley (UCB), to develop an initial preconceptual design for a small, modular 236-MW(thermal) pebble-bed (PB) fluoride salt–cooled, high-temperature reactor (FHR) (PB-FHR), as a part of a larger U.S. Department of Energy Integrated Research Project

(IRP) collaboration with Massachusetts Institute of Technology and University of Wisconsin–Madison to establish the technical basis to design, license, and commercially deploy FHRs. The key novel feature of this Mark-I PB-FHR (Mk1) design compared to previous FHR designs is the use of a nuclear air-Brayton combined cycle (NACC) based on a modified General Electric (GE) 7FB gas turbine (GT). This combination is designed to produce 100 MW(electric) of base-load electricity when operated with only nuclear heat and to increase the power output to

*E-mail: charalampos@berkeley.edu

242 MW(electric) by injecting natural gas (NG) (co-firing) for peak electricity generation. A full and detailed technical description is also available.¹ The key design parameters of the Mk1 PB-FHR are presented in Table I.

The primary purpose of the Mk1 design, with its co-firing capability, is to change the value proposition for nuclear power. The new value proposition arises from additional revenues earned by providing flexible grid support services in addition to base-load electrical power generation.

It is important to note the use of scaled experiments in the development of the design of the Mk1 PB-FHR. A better understanding of the basic phenomenology of high-Prandtl-number (Pr) coolant thermal hydraulics and pebble dynamics is possible through geometrically scaled experiments that employ a simulant fluid in place of the Mk1 PB-FHR reactor coolant.²

A summary of work contributing to the design—the design itself—are provided below, starting with a basic overview of the Mk1 PB-FHR, including its novel features and advantages. Subsequently, we describe the Mk1's neutronic design and aspects. We then successively describe its thermal-hydraulic phenomenology and performance, followed by the design of the Mk1's power conversion system, including its coiled tube air heaters

(CTAHs) and modified GT combined cycle. We finally conclude with a brief description of the Mk1's economics.

II. MK1 PB-FHR BASICS

Fluoride salt-cooled, high-temperature reactors combine several technologies from other reactor types. Key Mk1 operating parameters and design basics are as follows:

1. graphite pebble fuel compacts with coated-particle fuel
2. FLiBe (${}^7\text{Li}_2\text{BeF}_4$) molten salt coolant
3. inlet/outlet temperatures of 600°C/700°C
4. pool-type reactor at near atmospheric pressures.

The Mk1 is designed so that all components, including the reactor vessel, GT, and building structural modules, can be transported by rail, enabling modular construction. With these modules being fabricated in factories using computer-aided manufacturing methods, the assembly of a Mk1 at a reactor site will more closely resemble three-dimensional (3-D) printing than conventional nuclear construction. The design constraint of rail transport limits the width of all components, including the

TABLE I

Key Mk1 PB-FHR Design Parameters

Parameter	Value
Reactor design	
Thermal power [MW(thermal)]	236
Core inlet temperature (°C)	600
Core bulk-average outlet temperature (°C)	700
Primary coolant mass flow rate (100% power) (kg/s)	976
Primary coolant volumetric flow rate (100% power) (m ³ /s)	0.54
Power conversion	
GT model number	GE 7FB
Nominal ambient temperature (°C)	15
Elevation	Sea level
Compression ratio	18.52
Compressor outlet pressure (bar)	18.58
Compressor outlet temperature (°C)	418.7
Compressor outlet mass flow (total flow is 440.4 kg/s; conventional GE 7FB design uses excess for turbine blade cooling) (kg/s)	418.5
CTAH outlet temperature (°C)	670
Base-load net electrical power [MW(electric)]	100
Base-load thermal efficiency (%)	42.5
Co-firing turbine inlet temperature (°C)	1065
Co-firing net electrical power output [MW(electric)]	241.8
Co-firing efficiency (gas-to-peak-power) (%) ^a	66.4

^aThe co-firing efficiency is the ratio of the increased power produced (total minus base load) during peaking to the energy input from combustion of NG and represents the efficiency with which the NG combustion energy is converted into electricity.

reactor vessel, to <3.6 m, which in turn constrains the Mk1's thermal power. However, the constrained value matches well to the largest rail-shippable GTs now commercially available.

One key new characteristic of the Mk1 is that it eliminates the intermediate coolant loop used in all previous FHR designs and in all sodium-cooled fast reactors (SFRs) built to date, as shown in the flow schematic in Fig. 1. SFRs have used intermediate loops because sodium reacts energetically when contacted with water in a steam generator (as well as with air and carbon dioxide). However, the fluoride salt coolant used in FHRs has high chemical stability.³

For advanced reactors, the reactor vessel volume provides one metric for primary system cost. The Mk1 PB-FHR reactor vessel has a volumetric power density of 0.87 MW(electric)/m³. This is lower than typical pressurized water reactors (PWRs) [2.8 MW(electric)/m³] but is approximately three times larger than both the S-PRISM SFR [0.29 MW(electric)/m³] (Ref. 4), which uses a low-pressure (LP), pool-type vessel, and the Pebble-Bed Modular Reactor (PBMR) [0.24 MW(electric)/m³] (Ref. 5), which uses a high-pressure (HP) reactor vessel.

II.A. Nuclear Air-Brayton Combined Cycle

In the current fleet of nuclear power plants, designers try to maximize the thermal power of the reactor and subsequently couple an appropriate steam turbine/cycle. In the case of the NACC, the opposite applies; the GT capabilities determine the reactor thermal power. For the Mk1 baseline design of the NACC, a modified version of the GE 7FB GT is used. The GE 7FB is a rail-shippable, 60-Hz machine, already widely deployed in the United States. In its conventional, NG-only configuration, it supplies 183 MW(electric) in a simple cycle and 280 MW(electric) in a combined cycle. The NACC is also a hybrid power conversion system that allows supplementary firing with fossil fuels (gas/liquid) above the nuclear base-load heat with a tremendously high-power ramp rate of 24.5 MW/min to 69.3 MW/min, compared to the more typical 8 MW/min of a conventional GT (Ref. 6). This enables peak power production, as well as the ability to provide flexible capacity and several ancillary services to the grid. Among these are spinning reserve, black start services, peaking power, and frequency regulation. The performance of the Mk1 NACC design is summarized in

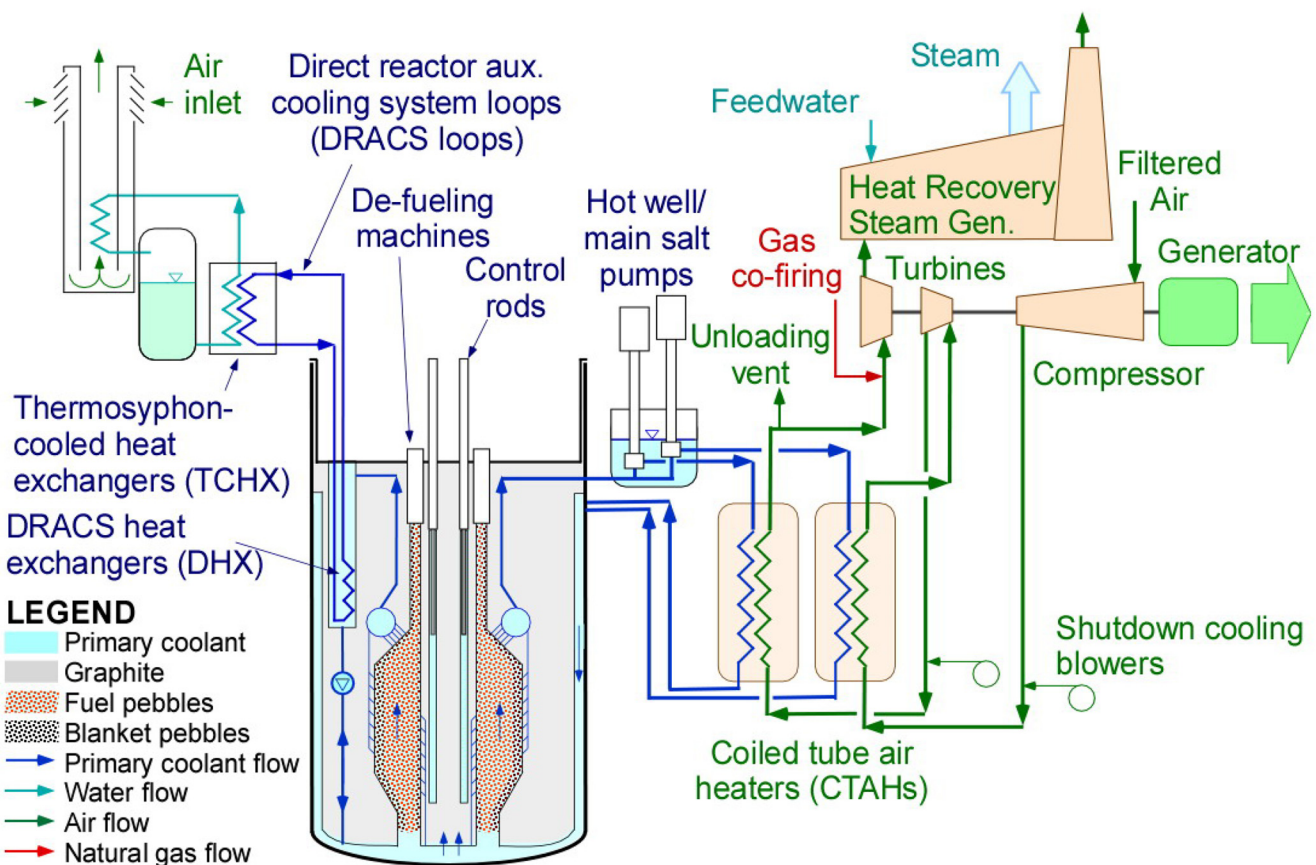


Fig. 1. Schematic of the Mk1 flow.

Table II. The design of the NACC was performed using GE's extensive technical literature, while performance was estimated using Thermoflow's THERMOFLEX®, a commercial power cycle modeling tool. Detailed design and performance estimation studies under nominal and off-nominal conditions of the NACC are provided by Andreades et al.^{7,8}

Another ability of the NACC is to decouple power conversion transients from the reactor due to the open cycle configuration. This reduces risks involved with loss-of-load events, for example, as the reactor will not feel this transient. This is accomplished by venting air to atmosphere past the last point of contact of the air stream with the primary loop, through an unloading vent, as shown in Figs. 1 and 2. The air mass flow seen by the primary heat exchangers remains relatively steady. Overcooling transients and the potential for salt freezing, present primarily during start-up due to the low initial compressor outlet temperature, are mitigated through electrical trace heating present in the primary heat exchangers.

The Mk1 PB-FHR uses two CTAHs to transfer heat from the main salt to pressurized air. Because of the

compact size of the Mk1 reactor vessel and main salt system, these CTAHs are located only 12.5 m from the centerline of the reactor vessel. Even though significant thermal expansion occurs when the reactor and main salt system are heated from their installation temperature to their normal operating temperature, the relatively short spacing between the reactor vessel and CTAHs allows this ~0.13-m expansion to be accommodated by placing the CTAHs on horizontal bearings and using bellows in the air ducts. This is similar to the approach taken to manage thermal expansion in the primary loop of conventional PWRs, where the steam generators are supported on vertical bearings and move horizontally in response to thermal expansion of the reactor hot- and cold-leg pipes.

II.B. Primary Coolant System

The Mk1 PB-FHR design is careful to minimize pressure losses in the primary coolant system. The nominal coolant flow rate in the Mk1 design is 0.54 m³/s, and nominal flow velocities are kept relatively low (~2.0 m/s) to keep the dynamic head relatively low. Keeping flow velocities below 2.0 m/s drove the high-level design of the Mk1 primary coolant system. Future work will entail detailed design, computational fluid dynamics (CFD) modeling, and scaled fluid dynamics experiments to reduce the salt inventory in the reactor, while keeping pressure losses in the system acceptably low.

Figure 3 shows the primary coolant flow paths under normal power and shutdown cooling operation. Thicker lines indicate main flow paths. Bypass flows are not shown for simplicity, although these will need to be quantified as they can have a significant effect on the behavior of the primary coolant loop and structural materials.

II.C. Normal and Safety Decay Heat Removal

The Mk1 PB-FHR uses the CTAHs for normal shutdown cooling and maintenance heat removal. For shutdown cooling, one or both main salt pumps are operated at low speed to circulate salt. A variable-speed blower system circulates ambient air through one or both of the CTAHs. The air flow rate is controlled to match the CTAH heat removal to the decay heat generation rate, and the salt flow rate is controlled to keep the salt cold-leg temperature constant at 600°C to minimize thermal stresses to the reactor vessel and core internals. Because the two CTAHs can be drained independently, for maintenance, a single CTAH can be drained while the other CTAH continues to provide shutdown cooling.

The direct reactor auxiliary cooling system (DRACS) is a natural-circulation-driven decay heat removal system

TABLE II

Mk1 NACC Operating Parameters at ISO Conditions*

Parameter	Value
P_{BL}/P_{CF} [MW(electric)]	100/241
P_{BL}/P_{CF} [MW(thermal)]	236/448
η_{BL} (%)	42.4
η_{CF} (net) (%)	53.8
η_{CF} (gas only) (%)	66.0
Power ramp rate (MW/min)	24.5 to 69.3

*BL = base load; CF = co-fired.

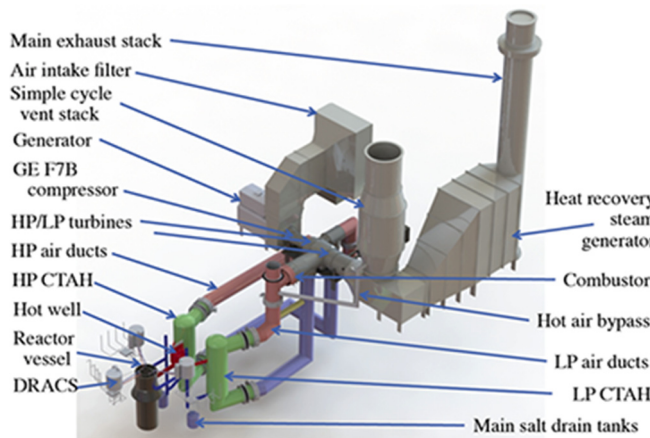


Fig. 2. The Mk1 PB-FHR interface with its NACC power conversion system.

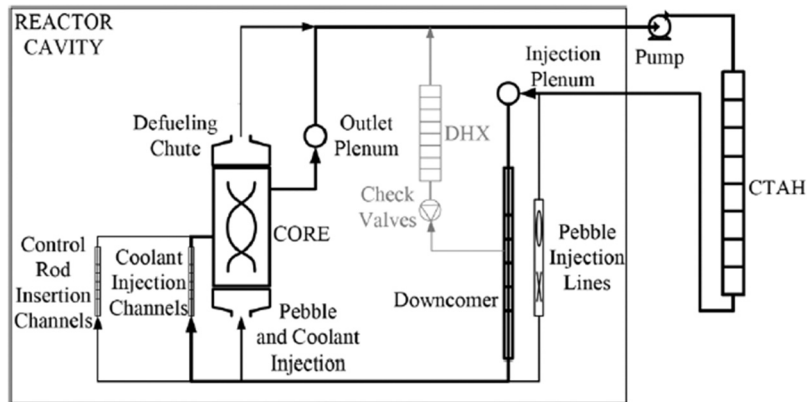


Fig. 3. Primary coolant flow paths under normal power and shutdown cooling operation.

consisting of three modular 50%-capacity DRACS loops. Each loop is capable of removing 1% of nominal shutdown power (2.36 MW). Further system design is needed to investigate safety and economic trade-offs between the number of loops in the system and each loop's heat removal capacity. The DRACS provides a diverse and redundant means to remove decay heat in the event that the normal shutdown cooling system does not function. The DRACS transfers heat to ambient air, which serves as the ultimate heat sink for decay heat. The DRACS coolant loop uses natural circulation to transfer heat from the DRACS heat exchanger (DHX) to a thermosyphon-cooled heat exchanger (TCHX). Heat is removed by convection and thermal radiation from the tubes of the TCHX to water-filled thermosyphon tubes, where water boils and transports heat to a natural draft, air-cooled condenser. The DRACS coolant is FLiBe to reduce the probability of the primary salt becoming contaminated with other salts due to heat-exchanger leaks.

For emergency decay heat removal through the DRACS, natural circulation is established in the primary system, with flow upward through the core, then downward through the DHX and downcomer. The DHX is designed to keep the salt cold-leg temperature constant at 600°C and a constant hot-leg temperature of 700°C assuming a decay heat-driven mass flow rate of ~10 kg/s. For these shell-side values, the tube side is estimated to have an inlet temperature of 526°C, an outlet temperature of 608°C, and a mass flow rate of ~12 kg/s. For design details see Ref. 9. During normal operation, the primary coolant flows in forced circulation upward through the core, and a small amount of coolant bypasses the core upward through the DHX and other core bypass paths. A fluidic diode can provide high flow resistance for upward flow through the DHX during forced convection, to limit parasitic heat losses, and low flow resistance for downward flow through the DHX during natural circulation. This function can also be served by a simple ball-type

check valve, with a negatively buoyant graphite and/or silicon carbide ball. A check valve with small allowable flow in the upward direction could provide precise and predictable flow loss coefficients in both flow directions. Figure 4 shows the coolant flow paths and bypass flows during forced-circulation and natural-circulation operation.

Each DRACS loop is fabricated and mounted into a frame that can be lifted by crane. A key issue for detailed design of the DRACS is the containment penetration barrier needed for horizontal legs and how to design hatches above the frame to allow loop installation and removal. The DRACS loop is not accessed under normal operation, so these hatches are designed to act as effective, passive missile barriers. Geometry constraints and reliable operation are the primary design constraints for the DRACS.

II.D. Balance of Plant

The Mk1 plant layout facilitates multimodule plant configurations. The configuration of the reactor and power conversion systems allows multiple PB-FHRs to be lined up in a row and to have a clear boundary between the reactor and vital safety areas and the balance of plant (BOP). The GT and associated equipment are configured

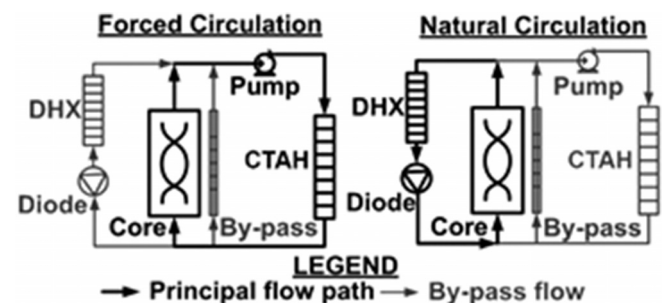


Fig. 4. FHR primary coolant flow paths for forced-circulation and natural-circulation operational modes.

to minimize the length of the air ducts and the associated pressure losses and circulating power while maintaining a clear boundary between the reactor and the BOP.

Most BOP components are off-the-shelf, and no modifications are needed to accommodate the NACC. One potential modification to BOP may be the NG supply system, which is a source of stored energy. Conventional NG safety standards are applied, as well as additional safety measures, e.g., double bleed and block valves in the NG supply lines, ventilation, and underground vaulted supply lines with controlled access, which are detailed in Ref. 8.

II.E. Plant Site Layout

Figure 2 provides an isometric view of a notional Mk1 single-unit arrangement. This 3-D computer-aided-design model was generated using input from all of the research described within this summary paper as well as expert input collected during four workshops hosted as part of the FHR-IRP (Refs. 10 through 14). A full 12-unit power plant site arrangement is depicted in Fig. 5. The heat recovery steam generators (HRSGs) and BOP are set at 90 deg to the GT in order to create a compact site arrangement and allow a clear separation boundary with the protected area. Spent-fuel storage pools and operating and auxiliary buildings are also shown. Lift towers are used

for modular and sequential or parallel construction of units, allowing for staggered operation and earlier revenues as units come online.

III. NEUTRONICS

The pebble-filled reactor core is annular, with an inner radius of 0.35 m and an outer radius of 1.25 m. Coolant flows upward and radially outward through the core, injected at the bottom and from the center graphite reflector cylinder. The core is surrounded by center and outer graphite reflector blocks. The lowermost and uppermost regions of the annular core are tapered chutes for fueling and defueling, respectively. Figure 6 presents a cross section of the reactor showing the core geometry.

There are two pebble regions within the pebble bed. The inner region, from radius 0.35 to 1.05 m, contains fuel pebbles. The outer region, from radius 1.05 to 1.25 m, contains inert graphite pebbles. The primary purpose of the graphite pebble reflector is to attenuate the fast-neutron flux at the outer solid graphite reflector so as to extend the outer reflector lifetime to the full plant lifetime. The resulting design has an active core volume of 10.4 m³ and a graphite pebble volume of 4.8 m³.

The annular geometry of the Mk1 pebble design, shown in Fig. 7, reduces the peak and average fuel temperatures of the pebbles by shortening the heat transfer

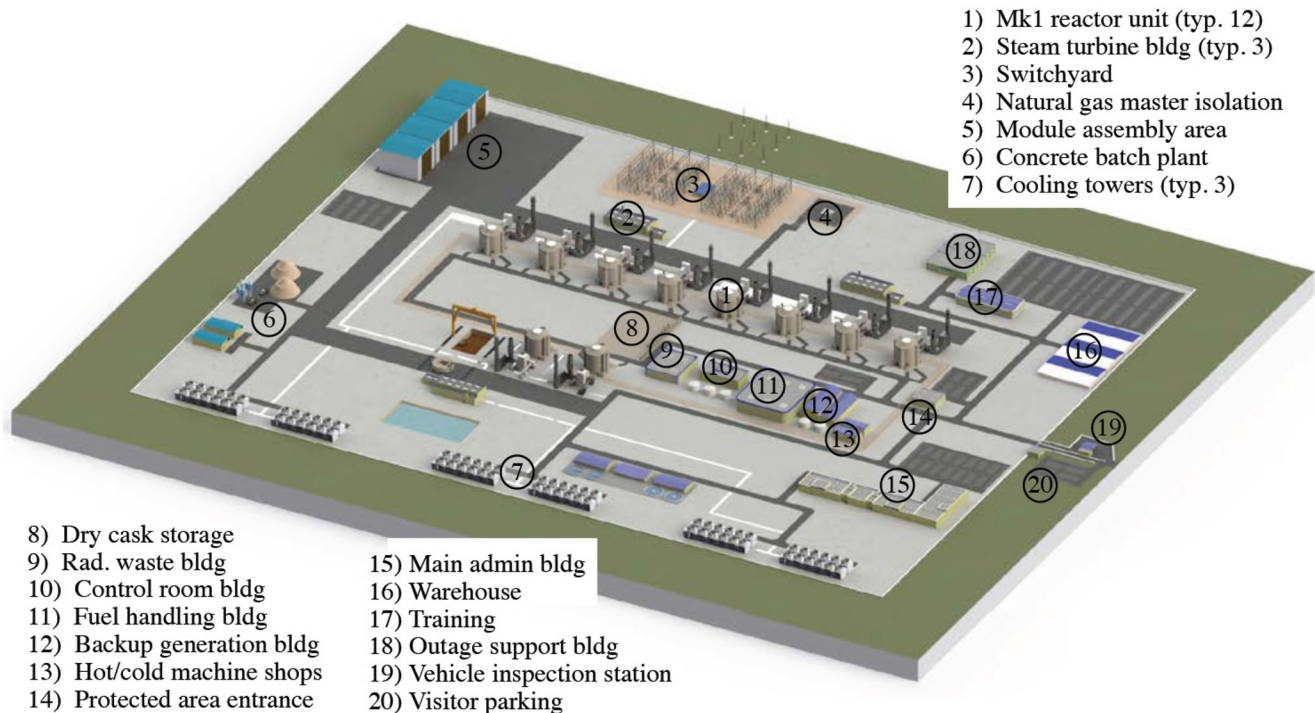


Fig. 5. Reference site arrangement for a 12-unit PB-FHR plant capable of producing 1200-MW(electric) base load and 2900-MW(electric) peak.

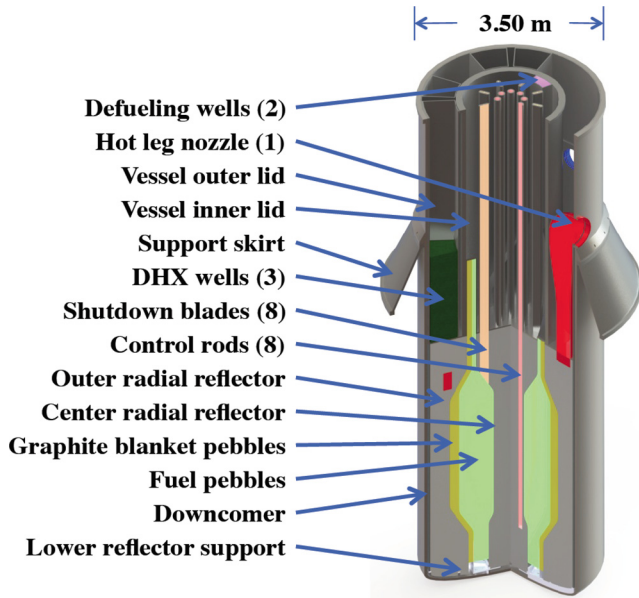


Fig. 6. The Mk1 PB-FHR reactor vessel.

path length from the fuel layer to the coolant, thus increasing the safety margin for transient accident behavior. Also, the annular design allows control of pebble buoyancy in the liquid salt coolant by adjusting the density of the central graphite core in the pebble. This design has a 1.5-mm-thick annular layer containing, on average, 4370 tristructural-isotropic (TRISO) particles. This layer surrounds a 12.5-mm-radius inert graphite kernel. A 1.0-mm-thick, high-density graphite protective layer encapsulates the entire fuel pebble. The details about the TRISO particle design are summarized in Table III, with the parameter estimates based on design studies for a 290-MW(thermal) core and scaled to a 236-MW(thermal) core.

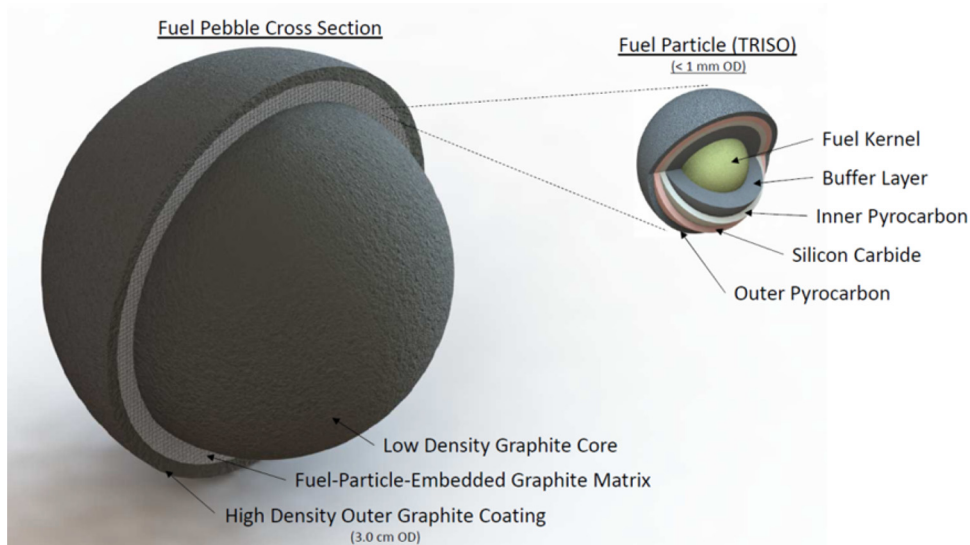


Fig. 7. Details of Mk1 fuel compact geometry and TRISO fuel particles.

III.A. Fuel Management

In the Mk1 design, fuel pebbles are continuously circulated through the core at a slow pace. The pebbles are introduced into the bottom of the pebble bed and rise up as pebbles are removed from the top of the bed at an approximate rate of 0.2 Hz. Fuel pebbles are introduced through four inner pebble injection channels, and blanket pebbles are introduced through four outer channels. Pebbles rely on their positive buoyancy in the coolant salt to move upward through the core and move in plug flow through the active region. Pebbles are removed at the top of the core through an annular slot that converges into two defueling machines. Pebbles are recirculated through the core approximately eight times before reaching their discharge burnup, which is 180 GWd/tonne U. With an average residence time of 2.1 months, each pebble is expected to spend 1.4 years in core.

III.B. Neutronics Modeling and Results

Current depletion studies of the FHR have relied on a combination of MCNP5 and ORIGEN modeling. A suite of Python-based tools was developed to manage an iterative search for equilibrium core composition accurately accounting for the complex core and pebble geometries. The suite of tools developed for the FHR core design include Burnup Equilibrium Analysis Utility (BEAU), FHR Input-deck Maker for Parametric Studies (FIMPS), and mocup.py (Ref. 15).

Multiphysics models with different levels of spatial resolution and fidelity have been developed for the Mk1 FHR transient behavior analysis, including a coupled

TABLE III
Mk1 PB-FHR TRISO Fuel Particle Design

Parameter	Value
Fuel kernel diameter (μm)	400
Fuel kernel density (kg/m^3)	10500
Fuel kernel composition	$\text{UC}_{1.5}\text{O}_{0.5}$
Buffer layer thickness (μm)	100
PyC inner layer thickness (μm)	35
SiC layer thickness (μm)	35
PyC outer layer thickness (μm)	35

reactor kinetics and heat transfer unit-cell model,¹⁶ a coupled neutron diffusion and porous media heat transfer full-core model,¹⁷ and a coupled full-core model based on the Monte Carlo code Serpent and the CFD code OpenFOAM (Ref. 18).

The first model is based on the point-kinetics equations with six groups of delayed neutrons and the lumped capacitance heat transfer equations. The model represents an average fuel pebble and FLiBe salt in 40% of the unit-cell volume. Unlike light water reactors (LWRs), FHRs have substantial graphite reflectors, whose thickness is comparable to the neutron mean-free-path length scales. To account for the reflector effect on neutron lifetime, additional (fictional) groups of delayed neutrons are added in the point-kinetics equations to represent the thermalized neutrons coming back from the reflectors. This work is made open source under this name: Python for Reactor Kinetics (PyRK) (pyrk.github.io).

The second model is based on a coupled neutron diffusion and finite element heat transfer model. The neutron energy spectrum is divided into eight energy groups. The group boundaries are chosen to capture the cross-section changes in heavy metals and in isotopes in the FLiBe salt. Multigroup cross sections and diffusion coefficients are generated using the Monte Carlo code Serpent and defined as input in COMSOL 5.0. A MATLAB package has been developed to automatically read data from Serpent output files and produce temperature-/density-dependent group constants for as many neutron energy groups as deemed necessary.

The third multiphysics code couples the Monte Carlo code Serpent-2 for neutron transport and the CFD code OpenFOAM for thermal hydraulics and the discrete element method for random pebble configurations.

Using 19.9% enriched uranium fuel, the attainable discharge burnup from the equilibrium core is calculated to be 180 GWd/tonne U, and the corresponding pebble residence time is 1.4 effective full-power years (EFPY).

The peak power density is $80 \text{ W}/\text{cm}^3$ while the bed average power density is $20 \text{ W}/\text{cm}^3$. Three out of eight control rods, located close to the periphery of the center graphite reflector, can keep the reactor subcritical at cold-zero-power condition. Likewise, four out of eight shutdown blades provide adequate shutdown margin when inserted into the bed of pebbles. Temperature coefficients of reactivity calculated for the Mk1 core are summarized in Table IV. While the fuel, graphite moderator, and coolant have strong negative temperature coefficients of reactivity, both center and outer graphite reflectors have small positive reactivity feedback. As the reflector temperature will strongly depend on the coolant temperature, the net reactivity effect of uniform coolant temperature increase is expected to be close to zero, when the graphite reflector temperature will equilibrate with the coolant temperature.

A preliminary estimate of the radiation damage to the center graphite reflector is 2.1 displacements per atom (dpa)/EFPY, implying ~ 10 -EFPY lifetime. The peak radiation damage to the outer solid graphite reflector is 0.03 dpa/EFPY, implying that there will be no need to replace this reflector over the FHR plant lifetime.

IV. THERMAL HYDRAULICS

This section provides a list of key thermal-hydraulic phenomena for FHR technology and presents a high-level overview of codes that have been used for thermal-hydraulic steady-state and accidental transient analyses of FHRs. This section then focuses on the experimental basis needed to identify FHR-specific phenomenology and validate FHR modeling codes. A more detailed version of this discussion is presented elsewhere.^{12,19}

IV.A. Key FHR Thermal-Hydraulic Phenomena

Fluoride salts are low-volatility fluids with high volumetric heat capacities, melting temperatures, and

TABLE IV
Mk1 Temperature Coefficients of Reactivity*

Component	Temperature Reactivity
Fuel (pcm/K)	-3.8
Coolant (pcm/K)	-1.8
Center graphite reflector (pcm/K)	+0.9
Graphite moderator (pcm/K)	-0.7
Outer graphite reflector (pcm/K)	+0.9

*Reference 15.

boiling temperatures. The differences in thermal-hydraulic phenomena in FHRs emerge from the differences in the thermophysical properties of the fluoride salts and the structural materials used with them, compared to other reactor coolants and their typical structural materials.

Fluoride salts have high volumetric heat capacities. The volumetric heat capacity of the primary coolant FLiBe exceeds even that of water ($4.18 \text{ MJ/m}^3 \cdot \text{K}$). Therefore, FHRs operate with lower primary coolant volumetric flow rates, pressure drops, and pumping power than LWRs. These FHR operating parameters are also much lower than those for SFRs and high-temperature gas-cooled reactors (HTGRs).

The fact that low volumetric flow rates of fluoride salts can transport large amounts of heat has many implications for the design of FHRs. For example, this characteristic makes fluoride salts particularly effective in passive, buoyancy-driven natural-circulation heat transfer.²⁰ For future FHR reactors to be commercially attractive, it is critical that FHR designers leverage the favorable thermophysical properties of the fluoride salts to the maximum degree possible while simultaneously mitigating the impacts of the nonfavorable properties, primarily the high freezing temperature of the fluoride salts.

Sections IV.A.1 through IV.A.4 review key thermal-hydraulic phenomena that arise from the unique thermophysical properties of the fluoride salts and FHR structural materials.

IV.A.1. High-Pr-Number Coolant

The thermal conductivity of the baseline FHR primary coolant FLiBe is greater than water. However, FLiBe is also a highly viscous fluid, thus making it a high-Pr-number fluid (~ 13 at 677°C). Most previous nuclear experience is with moderate Pr (~ 1 for water/helium) or low Pr ($\sim 10^{-3}$ for sodium).

The greater thermal conductivity of FLiBe creates the potential for achieving heat transfer coefficients comparable to those for water even though the viscosity of FLiBe is much higher. However, the high volumetric heat capacity of FLiBe means that FHR convective heat transfer commonly occurs at Reynolds numbers that result in laminar or transition regime flow even under forced circulation, and natural-circulation heat transfer is almost always in the transition or laminar regime. For this reason, unlike reactors using other coolants, FHR designs will commonly use enhanced heat transfer surfaces or small-diameter flow channels, such as those occurring in pebble beds.

IV.A.2. Potential for Freezing (Overcooling Transients)

Mixtures of fluoride salts have high freezing temperatures, typically between 320°C and 500°C , which makes overcooling transients an important topic for design and safety analysis. The 8-MW(thermal) Molten Salt Reactor Experiment (MSRE), which operated from 1965 to 1969, experienced freezing in its air-cooled radiator; the radiator was then thawed without damage.²¹ The lack of damage can be attributed in part to the particularly low volume change that the MSRE coolant salt, FLiBe, experiences upon freezing: $\sim 2.07\%$ (Ref. 22).

Moreover, buoyancy forces can lead to significant flow reorganization in porous media, such as the pebble-bed core and the shell side of twisted tube heat exchangers in FHRs (Ref. 20). Buoyancy forces are likely to be significant in FHRs as they operate at relatively low Reynolds numbers compared to water-cooled reactors, liquid metal-cooled reactors, or gas-cooled reactors. This makes FHRs resilient to high thermal gradients such as cold spots from overcooling or hot spots due to local power peaking.

IV.A.3. Bypass Flow

The graphite reflector blocks in the FHR can shrink and swell as complex functions of irradiation and temperature. These changes can lead to the formation of gaps between the blocks through which coolant will flow. The nature of this bypass flow must be carefully studied to assess the impact on temperature profiles within the reflector blocks. Bypass flows can have significant effects on the coolant outlet temperature gradient. For fast transients, especially, detailed temperature profiles of the coolant should be taken into account for thermal stress calculations on metallic structures outside the core.

IV.A.4. Radiative Heat Transfer

At high operating temperatures, radiative heat transfer to and from the reactor cavity, as well as total heat transfer to and from the reactor vessel, must be calculated. Likewise, wavelength-dependent absorption data are needed for coolant salts to allow their radiative interactions with heat transfer surfaces to be assessed.

IV.B. Thermal-Hydraulic Modeling

Numerous computer codes have been written to simulate the thermal-hydraulic characteristics of reactor cores and primary loops under steady-state and operational transient conditions, as well as potential accidents. New versions of some of these codes can be expected to be

developed, and efforts are now focused on adapting existing codes and developing new ones for the new generation of advanced LWRs as well as HTGRs. A similar capability is needed to properly model steady-state and transient thermal-hydraulic phenomena for the FHR, with an initial focus on design codes that will allow for rapid prototyping of the FHR system. The IRP is now focusing on developing models using two existing codes: RELAP5-3D and Flownex. These efforts are summarized here.

IV.B.1. RELAP5-3D Modeling

At this point on the development path of FHR technology, most thermal-hydraulic analyses have been performed using the RELAP5-3D systems analysis code. Although RELAP was originally developed for thermal-hydraulic analysis of LWRs and related experimental systems during loss-of-coolant accidents and operational transients, the code has recently been improved to simulate candidate Generation IV designs cooled by gas, supercritical water, and lead-bismuth. Liquid salt coolants, and more specifically FLiBe, have also been implemented into RELAP (Refs. 9 and 23), which allows it to model thermal-hydraulic steady-state and transient phenomena for the Mk1 PB-FHR.

Correlations for heat transfer and friction losses in the pebble-bed core can be manually implemented into the code, but a significant validation effort of these correlations is required. Because of its wide use in the nuclear industry for design and licensing of reactors, RELAP and sister codes like TRACE appear to be good candidates for simulation of FHR steady-state and transient responses. As an example, Galvez used RELAP to simulate the transient response of an earlier FHR design to a loss of forced circulation with scram²⁴ and used this model to optimize dimensions of the DRACS loop for a 900-MW(thermal) FHR. However, additional efforts are needed to properly account for all phenomena described in Sec. IV if RELAP and other thermal-hydraulic codes are to be used as the main system analysis codes for thermal-hydraulic behavior of the FHR, and a significant verification and validation (V&V) will be needed. Initial steps for such a process were taken in a UCB-hosted workshop.²⁵

IV.B.2. Flownex Modeling

Flownex is a one-dimensional thermal-fluids analysis software whose main purpose is to model thermal-hydraulic systems.²⁶ Flownex was used to model several systems in the PBMR, including the main power system and several supporting subsystems. Both transients and

steady-state cases were studied. Flownex was partially verified and validated against other codes for the PBMR, but no such effort has been undertaken for FHRs. Benchmarking Flownex against other codes and experimental data will be very valuable in terms of code V&V.

In parallel with RELAP5-3D, Flownex will be used to model the PB-FHR thermal-hydraulic systems and subsystems, including the main salt loop and the DRACS. A detailed estimate of salt volumes and salt flow paths is required to do this. Efforts are under way to quantify salt volumes and outline flow paths both within the reactor vessel and outside it. The Flownex model can be enhanced by appending the NACC on the secondary side of the CTAHs.

Single-phase natural circulation is an important mechanism that transfers decay heat from the core to the environment via the DRACS. Therefore, accurate modeling of single-phase natural circulation in both RELAP and Flownex is crucial. Simple natural-circulation loops can be modeled analytically and, using Flownex and RELAP and relevant system response metrics, such as mass flow rates and temperatures, can be compared. Such efforts are ongoing with models based on an experimental test loop built at UCB: the Compact Integral Effects Test (CIET) Test Bay, described in Sec. IV.C.2. Preliminary results from this V&V study indicate that RELAP is an appropriate tool to model the CIET Test Bay as a first step toward predicting the performance of the passive decay heat removal system of FHRs, with the code showing agreement within 5% with analytical predictions and within 10% with experimental data for natural circulation in the laminar regime and agreement within 8% with analytical solutions and within 25% with experimental data in the transition regime.⁹

IV.C. Integral Effects Tests for Thermal-Hydraulic Model Validation

Although preliminary thermal-hydraulic modeling of the FHR has been performed with systems analysis codes, these codes in their current state are not capable of capturing some of the key FHR thermal-hydraulic phenomena. Significant V&V efforts are therefore needed to increase the reliability of these codes to properly model thermal-hydraulic phenomena for the FHR. Some of these efforts are presented here.

IV.C.1. Scaling and the Use of Simulant Fluids

Thermal-hydraulic transient phenomena associated with FHR response to licensing-basis events (LBEs) evolve over brief time periods of minutes to days. Therefore, the

major constraint on experiments is not duration but rather scale because of the impracticality of performing integral effects tests (IETs) at the full-power level of the reactor. The major importance of geometric and power scaling was recognized in earlier studies of FHRs (Ref. 27).

Liquid salts are unique reactor coolants because simulant fluids can replicate salt fluid mechanics and heat transfer phenomena at reduced length scales, temperatures, and heater and pumping power, with low scaling distortion. UCB has identified a class of heat transfer oils that, at relatively low temperatures (50°C to 120°C), match the Pr, Reynolds, and Grashof numbers of the major liquid salts simultaneously, at ~50% geometric scale and heater power under 2% of prototypical values.²

Experiments have shown that the Pr numbers of Dowtherm A, which is a commonly used heat transfer oil, match those of FLiBe for certain temperature ranges. Specifically, the Pr of FLiBe throughout the expected Mk1 operating temperatures (600°C to 700°C) can be matched by Dowtherm A with a much lower temperature range (57°C to 117°C) (Ref. 3). The availability of such simulant fluids significantly reduces the cost and difficulty of performing IETs required for system modeling code validation for reactor licensing compared to working at prototypical temperatures and power levels with the actual coolant. Thus, the key IET experimental facilities needed to validate the FHR transient analysis codes can be university-scale facilities built and operated during the preconceptual design phase for FHR technology. Two of these facilities, operated at UCB, are described here.

IV.C.2. CIET Test Bay

The CIET Test Bay is a scaled-height, reduced-flow-area loop that reproduces the integral thermal-hydraulic response of the FHR primary coolant flow circuit using Dowtherm A. In the CIET Test Bay, heat is added to the fluid through an annular, electrically heated pipe and removed through water-cooled heat exchangers. Mass flow rates and bulk fluid temperatures along the loop are collected at various levels of heat input. The facility can run in both steady-state and transient modes to model the performance of the primary loop of FHRs under a defined set of LBEs. More details can be found elsewhere.²⁰

The CIET Test Bay has also provided data for V&V efforts and was instrumental in providing experience with operation and maintenance of components to be used on the CIET Facility, which is described in Sec. IV.C.3.

IV.C.3. CIET 1.0 Facility

To reproduce the integral transient thermal-hydraulic response of FHRs under forced- and natural-circulation operation, UCB has designed the CIET 1.0 Facility. CIET provides validation data to confirm the predicted performance of the DRACS under a set of reference LBEs. Using Dowtherm A at reduced geometric and power scales, test loops for CIET are fabricated from stainless steel tubing and welded fittings, allowing rapid construction and design modifications. The simplicity of the construction, compared to the complexity and safety requirements for tests with the prototypical salt, was a key element in enabling the experiments to be performed at lower cost than previous IETs for other types of reactors. Fluid flow paths in CIET replicate those in the FHR shown in Fig. 2. The CIET Facility is depicted in Fig. 8.

The research program for CIET has been completed as follows, with specific objectives associated with each step:

1. isothermal, forced-circulation flow around the loop, with pressure data collection to determine friction losses in the system
2. steady-state forced and coupled natural circulation in the primary loop and the DRACS loop
3. thermal transients: start-up, shutdown, and loss of forced circulation with scram.

In the future, additional transients will be completed under the research program, such as loss-of-heat-sink



Fig. 8. UCB CIET IET Facility.

transients. Further, the instrumentation and control system for CIET will be improved and will include reactor dynamics and power conversion models to more accurately model the integral performance of an FHR within a power plant. This will allow for the detailed study and optimization of the security and control strategy for FHRs.

More details about the design of the CIET Facility can be found elsewhere.⁹

V. POWER CONVERSION SYSTEM

The Mk1 design uses a NACC for its power conversion system. An overview of the system can be found in [Sec. II.A](#). This section provides details of specific Mk1 NACC components.

V.A. Coiled Tube Air Heaters

The Mk1 PB-FHR design has two CTAHs, which transfer heat from the primary salt to compressed air from the GT system. The CTAHs are located below grade in the filtered confinement volume, immediately adjacent to the PB-FHR reactor cavity. The CTAHs use an annular tube bundle formed by coiled tubes with air flowing radially outward over the tubes, as shown in [Fig. 9](#).

The coiled tube assembly of each CTAH is located in a vertical cylindrical steel pressure vessel that is insulated on the inside to allow the vessel to operate at near room temperature. The air temperatures in the CTAHs are comparable to air temperatures inside modern HRSGs for natural gas combined cycle (NGCC) plants, so the design of the insulation system can draw upon this experience base.

Each CTAH uses inlet and outlet manifold systems that distribute the liquid flow into and out of the coiled tubes. The inlet manifolds consist of four vertical hot liquid manifold pipes that enter from the top of the vessel

and extend downward along the outside of the coiled tubes. The Mk1 hot manifold pipes are 0.320 m in outside diameter with a 0.020-m-thick wall, and the cold manifold pipes are 0.215 m in outside diameter with a 0.020-m-thick wall. At each tube row elevation in the coiled tube bank, hot liquid is supplied into multiple tubes that then wrap around the coiled bundle, forming a single “lane” of tubes at that elevation that wraps around the tube bank one or more times. Likewise, at the center of the tube bundle, there are four vertical cool liquid manifold pipes that receive the flow from the tubes and direct it downward and out of the heater vessel.

The Transverse Heat Exchange Effectiveness Model (THEEM), a finite volume simulation code, is being developed at UCB to estimate the CTAH’s performance and effectiveness and in turn to optimize its overall design.²⁸

V.B. Power Conversion and Turbine

To implement nuclear heating, the Mk1 NACC design modifies the GE 7FB GT as shown in [Fig. 10](#). Flow through the NACC system occurs as follows:

1. Air intake occurs through a filter bank, and the air is compressed to a pressure ratio of 18.5. For a nominal 15°C, 1.01-bar ambient condition, the air exits the compressor at a temperature of 418°C.

2. After the compressor outlet, the air passes through a HP CTAH and is heated up to a turbine inlet temperature of 670°C. The air is then expanded to approximately the same temperature as the compressor outlet temperature: 418°C. This criterion determines the expansion ratio of the first expansion stage at nominal design conditions.

3. The air is then reheated back up to 670°C by passing through a second LP CTAH. It is important to design this LP external heating system to have minimum

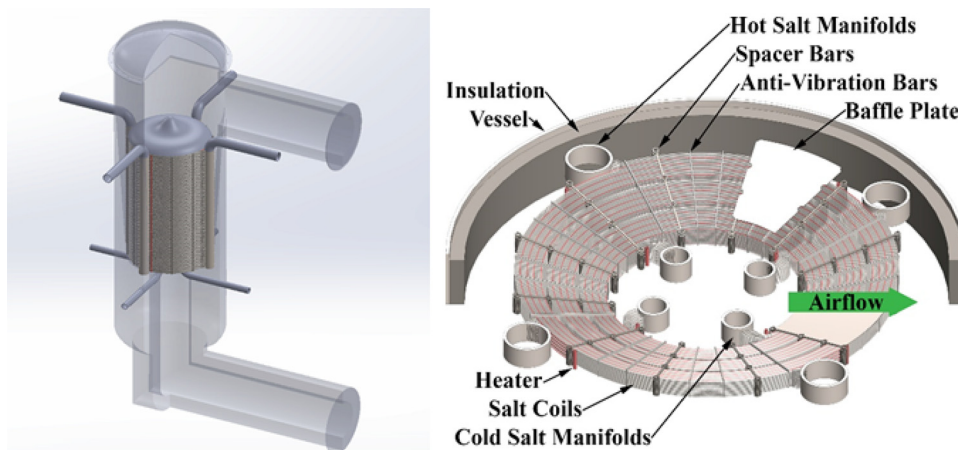


Fig. 9. Isometric view of the CTAH assembly and subbundle 3-D model with major components labeled.

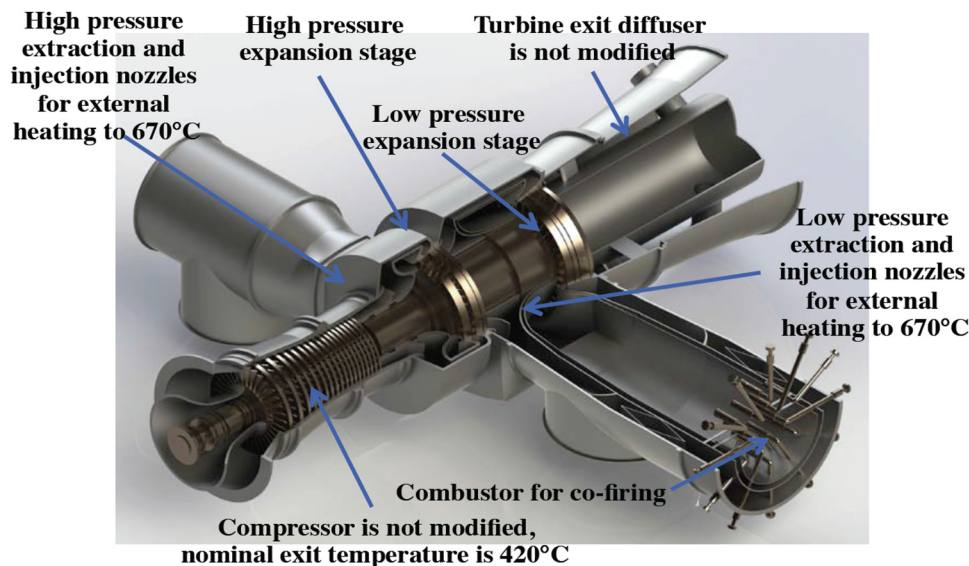


Fig. 10. Cross section of the modified GE 7FB GT used for power conversion in the Mk1 PB-FHR.

pressure drop in order to achieve acceptable circulating power loss and cycle efficiency.

4. After the LP CTAH, the air is above the autoignition temperature of NG. To provide power peaking, a fuel such as NG can be injected and burned to increase the turbine inlet temperature and the power output.

5. The heated air is then expanded down to nearly atmospheric pressure and 395°C to 700°C, depending on the peak power level, by passing through an additional set of LP turbine blades, before entering the HRSG. The HRSG must be designed to accommodate a relatively wide range of air inlet temperatures due to the large change that occurs between low-carbon base-load operation and peak power operation with NG injection.

Reheat and external firing are both proven technologies and are commercially available on large industrial GTs (e.g., Alstom GT11N2 and Alstom GT24). The main modifications needed to accommodate nuclear heat for the GE 7FB GT include an extended shaft to accommodate reheat and a redesigned casing.

VI. TRITIUM MANAGEMENT

Neutron irradiation of the coolant produces tritium (^3H) by transmutation of ^6Li , and it produces ^6Li by transmutation of ^9Be . Tritium is a low-energy beta emitter, and it has a decay half-life of 12 years and a biological half-life of 10 days. At high temperature, H_2 has high diffusivity through metals and metal alloys, so it readily diffuses through the high-surface-area metal heat exchangers as well as through piping and vessel

walls. In order to control tritium emissions to the atmosphere, permeation barriers and capture methods are being studied.^{29,30}

Several tritium capture methods for the FHR are in the early stages of development: absorption in the graphitic fuel element, inert gas sparging, metallic membrane permeators, solid absorber beds, double-wall heat exchangers with a sweep gas or a removable solid getter in the intermediary space. Tritium permeation barriers for metallic heat-exchanger tubes are being studied in order to increase the maximum concentration of tritium that can be tolerated on the salt side in the salt-to-air heat exchanger while meeting the design limits for the atmospheric release of tritium.

Tritium absorption on the graphite fuel elements is an inherent feature of FHRs that may prove to be a highly effective tritium sink. At 600°C and above, hydrogen isotope absorption on graphite occurs through chemisorption. If all of the tritium produced by the Mk1 were to be absorbed on the pebble and graphite fuel in the 1.4 years before discharge, then a loading of 2 to 10 parts per million by weight T/C would be achieved (depending on the initial enrichment of ^7Li in the coolant). Based on high-temperature absorption data from the gas phase onto nuclear graphite, this loading is likely to be achievable. However, it needs to be understood if tritium absorption in the fuel elements will be a transport-limited or a solubility-limited process, and data need to be collected with irradiated and unirradiated graphite matrix material that constitutes the fuel. Furthermore, hydrogen absorption data from the salt melt are needed in order to capture the role of salt chemistry and the transport across the

salt-graphite interface. University of Wisconsin–Madison has active research in these areas.^{29–31}

VII. MK1 ECONOMICS

One of the critical questions about commercialization of a nuclear project is its economic and financial performance compared to its competitors. The Mk1 provides an interesting value proposition as an enabling technology for a low-carbon electricity grid with its ability to provide flexible capacity on demand and generate revenue from multiple streams. The costs of the Mk1 were estimated using a combination of top-down and bottom-up approaches. Capital costs were estimated using an inventory of major classes of materials and scaling their cost to those of known conventional systems. An overall capital cost of \$4500/kW to \$5093/kW base load was estimated depending on the number of units, ranging from 1 to 12, present at the power plant site. Having more units on site spreads out fixed costs and reduces the specific cost. When comparing the Mk1 to other plants, it is important to take into account its ability to produce added electricity at essentially no additional capital cost since all infrastructure required is already present and accounted for, which reduces the specific capital to \$1870/kW to \$2133/kW base load plus peaking. Similar to capital construction costs, operations and maintenance costs drop from \$81.05/MW-h (8.1 ¢/kW-h) to \$39.82/MWh (3.98 ¢/kW-h) as the number of units per site increases from 1 to 12.

In terms of revenue, the Mk1 performs favorably in various economic scenarios, with the main inputs that affect profitability being electricity price, NG price, and discount rate. These all point to possible ways to mitigate the Mk1’s investment risk, such as long-term NG or combustible fuel contracts and improved construction and supply chain management, in order to make it a more attractive venture. Finally, a comparison between the Mk1 and two different NGCCs (utility owned and merchant owned) demonstrates favorable performance of the Mk1 compared to both alternatives. The Mk1 maintains profitability under a wide range of NG prices. It remains competitive with NGCCs under low NG prices and becomes a much more attractive investment in markets where NG prices are high compared to the NGCCs, as NG costs drive NGCC performance, as depicted in Fig. 11. The net present value (NPV) and return on investment of the Mk1, which are key profitability metrics, remain positive in the assumed low, base, and high NG price scenarios, while NGCCs remain profitable only with low NG prices if electricity prices remain constant. This is similarly reflected in the levelized cost of electricity, where NG is a major cost driver for the NGCCs, while it has a less pronounced effect for the Mk1. The Mk1 produces less power more efficiently through NG compared to NGCCs and is therefore less affected by NG price swings. Finally, the NG price breakeven point suggests that the Mk1 can remain profitable to about twice or more the NG price of NGCCs, as fuel costs increase.

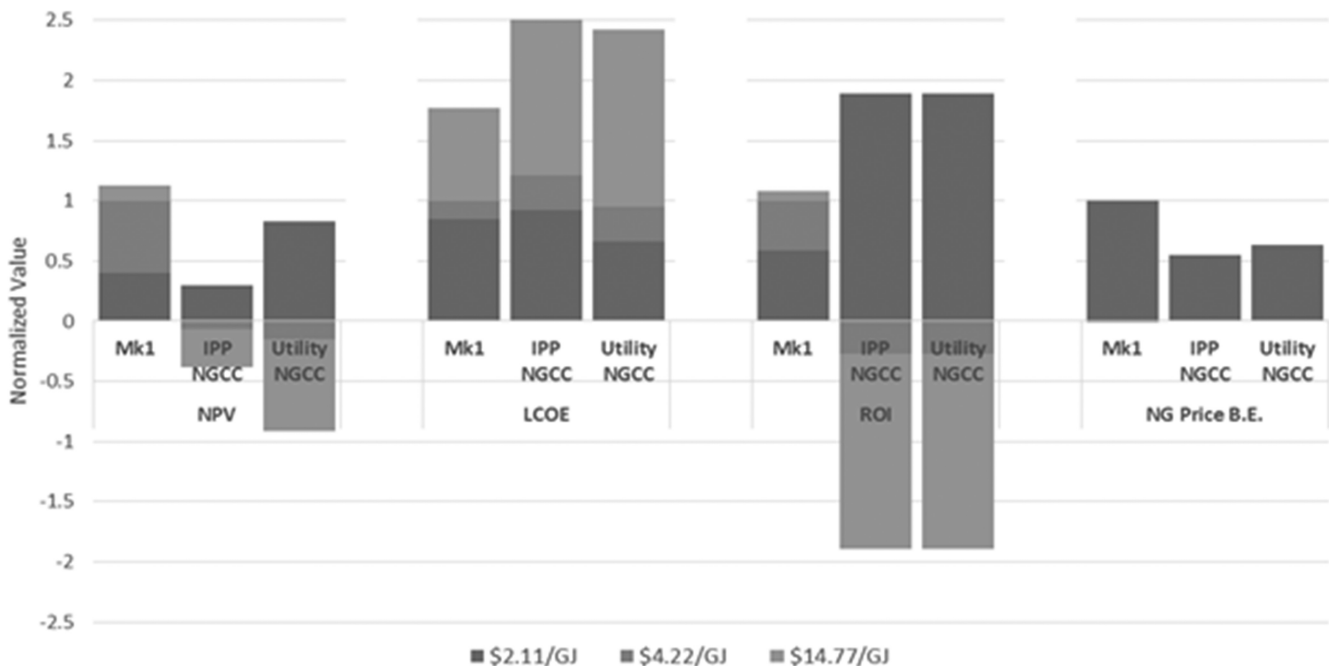


Fig. 11. Normalized financial parameters under NG price variation.

VIII. CONCLUSIONS

This summary paper presents a brief overview of past and ongoing research related to FHR-enabling topics at UCB. Various 3-D models of components and systems for the Mk1 PB-FHR plant are also presented. A more in-depth look at the technical aspects, including code development, materials issues, licensing strategies, and technology development road maps, can be found elsewhere in works produced by the member institutions of the FHR IRP (Refs. 1, 10, 11, and 13).

Acknowledgments

This research was performed using funding received from the U.S. Department of Energy Office of Nuclear Energy's Nuclear Energy University Programs.

References

1. C. ANDREADES and P. PETERSON, "Technical Description of the 'Mark I' Pebble-Bed Fluoride-Salt-Cooled High-Temperature Reactor (PB-FHR) Power Plant, UCBTH-14-002," University of California, Berkeley, Department of Nuclear Engineering (2014).
2. P. M. BARDET and P. F. PETERSON, "Options for Scaled Experiments for High Temperature Liquid Salt and Helium Fluid Mechanics and Convective Heat Transfer," *Nucl. Technol.*, **163**, 344 (2008); <http://dx.doi.org/10.13182/NT163-344>.
3. L. A. MANN, "ART Accident Analysis Hazards Tests (U)," ORNL-55-22-100, Oak Ridge National Laboratory (1955).
4. C. E. BOARDMAN et al., "A Description of the S-PRISM Plant," *Proc. Int. Conf. Nuclear Engineering*, Baltimore, Maryland, April 2–6, 2000, Vol. 8, ASME (2000).
5. E. J. SLABBER, "Technical Description of the PBMR Demonstration Power Plant," PBMR-016959, Rev. 4 (2006).
6. C. ANDREADES, "Nuclear Air-Brayton Combined Cycle Power Conversion Design, Physical Performance Estimation and Economic Assessment," Dissertation, University of California, Berkeley (2015).
7. C. ANDREADES et al., "Reheat Air-Brayton Combined Cycle (RACC) Power Conversion Design and Performance Under Nominal Ambient Conditions," *J. Eng. Gas Turbines Power*, **136**, 6, 062001 (June 2014); <http://dx.doi.org/10.1115/1.4026506>.
8. C. ANDREADES, L. DEMPSEY, and P. PETERSON, "Reheat Air-Brayton Combined Cycle Power Conversion Off-Nominal and Transient Performance," *J. Eng. Gas Turbines Power*, **136**, 7, 071703 (2014); <http://dx.doi.org/10.1115/1.4026612>.
9. N. ZWEIBAUM, "Experimental Validation of Passive Safety System Models: Application to Design and Optimization of Fluoride-Salt-Cooled, High-Temperature Reactors," PhD Thesis, University of California, Berkeley (2015).
10. "Fluoride-Salt-Cooled High Temperature Reactor (FHR) Materials, Fuels and Components White Paper," UCBTH-12-003, University of California, Berkeley, Thermal Hydraulics Laboratory (July 2013).
11. "Fluoride-Salt-Cooled, High-Temperature Reactor (FHR) Development Roadmap and Test Reactor Performance Requirements White Paper," UCBTH-12-004, University of California, Berkeley, Thermal Hydraulics Laboratory (June 2013).
12. "Fluoride-Salt-Cooled, High-Temperature Reactor (FHR) Methods and Experiments Program White Paper," UCBTH-12-002, University of California, Berkeley, Thermal Hydraulics Laboratory (May 2013).
13. "Fluoride-Salt-Cooled, High-Temperature Reactor (FHR) Subsystems Definition, Functional Requirement Definition, and Licensing Basis Event (LBE) Identification White Paper," UCBTH-12-001, University of California, Berkeley, Thermal Hydraulics Laboratory (Aug. 2013).
14. J. ROOT et al., "Structural Design and Modular Construction Approach for the Mk1 PB-FHR: NE 170—Senior Design Project (UCBTH-14-003)," University of California, Berkeley, Thermal Hydraulics Laboratory (June 20, 2014).
15. A. T. CISNEROS, "Pebble Bed Reactors Design Optimization Methods and Their Application to the Pebble Bed Fluoride Salt Cooled High Temperature Reactor (PB-FHR)," PhD Thesis, University of California, Berkeley (2013).
16. X. WANG et al., "A Sensitivity Study of a Coupled Kinetics and Thermal-Hydraulics Model for Fluoride-Salt-Cooled, High-Temperature Reactor (FHR) Transient Analysis," presented at ICAPP 2016, San Francisco, California, April 17–20, 2016.
17. X. WANG et al., "Coupled Reactor Kinetics and Heat Transfer Model for Nuclear Reactor Transient Analysis," presented at 24th Int. Conf. Nuclear Engineering, Charlotte, North Carolina, June 26–30, 2016.
18. M. AUFIERO and M. FRATONI, "Development of Multiphysics Models for Fluoride-Cooled High Temperature Reactors," *Proc. PHYSOR 2016*, Sun Valley, Idaho, May 1–5, 2016, American Nuclear Society (2016).
19. N. ZWEIBAUM et al., "Phenomenology, Methods and Experimental Program for Fluoride-Salt-Cooled, High-Temperature Reactors (FHRs)," *Prog. Nucl. Energy*, **77**, 390 (2014); <http://dx.doi.org/10.1016/j.pnucene.2014.04.008>.

20. R. O. SCARLAT, "Design of Complex Systems to Achieve Passive Safety: Natural Circulation Cooling of Liquid Salt Pebble Bed Reactors by Design," PhD Thesis, University of California, Berkeley (2012).
21. R. B. BRIGGS, "Molten-Salt Reactor Program: Semiannual Progress Report For Period Ending August 31, 1966," ORNL-4037, Oak Ridge National Laboratory (1967).
22. R. E. THOMA, "Chemical Aspects of MSRE Operations," ORNL-4658, p. 116, Oak Ridge National Laboratory (1971).
23. C. B. DAVIS, "Implementation of Molten Salt Properties into RELAP5-3D/ATHENA," INEEL/EXT-05-02658, Idaho National Laboratory (2005).
24. C. GALVEZ, "Design and Transient Analysis of Passive Safety Cooling Systems for Advanced Nuclear Reactors," PhD Thesis, University of California, Berkeley (2011).
25. "Fluoride-Salt-Cooled, High-Temperature Reactor Code Benchmarking White Paper," University of California, Berkeley, Thermal Hydraulics Laboratory (2015).
26. "Flownex SE: Nuclear," M-Tech Industrial (2013).
27. E. D. BLANFORD and P. F. PETERSON, "Global Scaling Analysis for the Pebble Bed Advanced High Temperature Reactor," *Proc. 13th Int. Topl. Mtg. Nuclear Reactor Thermal Hydraulics*, Kanazawa, Japan, September 27–October 2, 2009.
28. A. GREENOP and P. F. PETERSON, "Computer Modeling and Experimental Validation for Coiled-Tube Gas Heaters," *Proc. Int. Congress Advances in Nuclear Power Plants*, San Francisco, California, April 17–20, 2016, American Nuclear Society (2016).
29. M. YOUNG, H. WU, and R. SCARLAT, "Characterization of Tritium Transport in the Flibe-Graphite System, for In-Situ Tritium Absorption by the Fuel Elements of the Fluoride-Salt-Cooled High-Temperature Reactor (FHR)," *Proc. Int. Topl. Mtg. Nuclear Reactor Thermal Hydraulics (NURETH-16)*, Chicago, Illinois, August 30–September 4, 2015, American Nuclear Society (2015).
30. C. W. FORSBERG et al., "Tritium Control and Capture in Salt-Cooled Fission and Fusion Reactors," *Proc. 11th Int. Conf. Tritium Science and Technology*, Charleston, South Carolina, April 17–22, 2016, American Nuclear Society (2016).
31. H. WU et al., "Measurements of Fluoride Salt Intrusion in Matrix Graphite and High Purity Nuclear Graphite," *Proc. Int. Congress Advances in Nuclear Power Plants (ICAPP 2015)*, Nice, France, May 3–6, 2015.